Toxicology 445 (2020) 152603

Contents lists available at ScienceDirect

Toxicology

journal homepage: www.elsevier.com/locate/toxicol

Proteomic analysis of the cellular response to a potent sensitiser unveils the dynamics of haptenation in living cells

Erika Parkinson [a,b,1], Maja Aleksic [c,1,*], Predrag Kukic [c], Alistair Bailey [a,b], Richard Cubberley [c], Paul Skipp [a,b]

[a] Biological Sciences, University of Southampton, Southampton, SO17 1BJ, UK
[b] Centre for Proteomic Research, Institute for Life Sciences, University of Southampton, Southampton, SO17 1BJ, UK
[c] Safety & Environmental Assurance Centre, Unilever, Colworth Science Park, Sharnbrook, MK44 1LQ, UK

ARTICLE INFO

Keywords:
Allergic contact dermatitis
Cellular response
DNCB
Proteomics
Sensitisation
Haptenation

ABSTRACT

Haptenation of model nucleophiles, representing the key MIE in skin sensitisation, is routinely measured *in chemico* to provide data for skin allergy risk assessment. Better understanding of the dynamics of haptenation in human skin could provide the metrics required to improve determination of sensitiser potency for risk assessment of chemicals. We have previously demonstrated the applicability and sensitivity of the dual stable isotope labelling approach to detect low level haptenation in complex mixtures of proteins. In the present study, we investigated haptenation in a relevant living cell model over time at a subtoxic concentration. DNCB, an extremely potent sensitiser, caused minimal changes in overall protein differential expression in HaCaT cells and haptenated approximately 0.25 % of all available nucleophiles when applied at a subtoxic concentration (10μM) for 4 h. The data shows that the maximum level of haptenation occurs at 2 h and that DNCB, whilst being a promiscuous hapten, shows a preference for Cys residues, despite the considerably higher concentration of amine-based nucleophiles. Although a proportion of highly abundant proteins were haptenated, numerous haptenated sites were also detected on low abundant proteins. Certain proteins were modified at residues buried deep inside the protein structure which are less accessible to haptenation compared with surface exposed nucleophiles. The microenvironment of the buried residues may be a result of several factors influencing the reactivity of both the target nucleophile and the hapten.

1. Introduction

Electrophilic reactivity of chemicals (haptens), either direct or metabolically/oxidatively acquired, has long been established as prerequisite for induction of skin sensitisation (Lepoittevin, 2006; Natsch and Emter, 2017). Haptenation (covalent modification by small molecules) is termed the Molecular Initiating Event (MIE) in skin sensitisation (OECD, 2014). Covalently bound to skin proteins, small chemicals are seen by the immune system as antigens which trigger a clonal expansion of memory T cells specific to the hapten, resulting in sensitisation of an individual (OECD, 2014). Upon subsequent hapten exposure, the specific memory of the immune system is called upon and the skin site is infiltrated with the T cells eliciting localised inflammation (redness, oedema, itching), referred to as allergic contact dermatitis (ACD).

ACD is a common condition affecting approximately one fifth of the general population (Alinaghi et al., 2019). Haptens are ubiquitous in nature as well as components of cosmetic, household and medicinal products, resulting in exposure of large sections of the population. Historically, animal tests were used to determine levels of chemicals in products likely to sensitise (Basketter et al., 2001; Buehler, 1965; Kimber et al., 2002; Magnusson and Kligman, 1970; Robinson et al., 1990; van Och et al., 2001). In an era of Next Generation Risk Assessments (NGRA) (Dent et al., 2018; Luijten et al., 2020) without animal tests, skin sensitisation remains a high priority for the industry and relies on understanding the molecular mechanisms of sensitisation. Qualitative and quantitative characterisation of haptenation of skin proteins is a key step towards building better tools for use in NGRA (Baltazar et al., 2020; Natsch and Emter, 2017; Reynolds et al., 2019).

Studies on chemical reactivity have largely been conducted *in*

* Corresponding author at: Safety and Environmental Assurance Centre, Unilever, Colworth Science Park, Sharnbrook, Bedfordshire, MK44 1LQ, UK.
E-mail address: maja.aleksic@unilever.com (M. Aleksic).
[1] These authors contributed equally to this manuscript.

https://doi.org/10.1016/j.tox.2020.152603
Received 9 July 2020; Received in revised form 22 September 2020; Accepted 23 September 2020
Available online 28 September 2020

chemico, using small nucleophiles, amino acids and naturally occurring or synthetic peptides as models for proteins (Aleksic et al., 2009; Chipinda et al., 2010, 2014; Chittiboyina et al., 2015; Gerberick et al., 2004, 2007; Sanderson et al., 2016). Consequently, our knowledge on haptenation is substantially biased towards understanding reactivity of chemicals toward model nucleophiles rather than skin proteins and other cellular nucleophiles they haptenate *in vivo*. Since the advances in proteome analyses and ever more sensitive mass spectrometry instrumentation, simple models have been superseded by single proteins or relevant protein mixtures (Aleksic et al., 2007, 2008; Alvarez-Sanchez et al., 2004; Henriot et al., 2001; Parkinson et al., 2014). Sporadic studies have also addressed haptenation in cells and tissues following exposure to haptens. Utilising fluorescence of adducts combined with mass spectrometry, basal epidermal keratin pair K5/K14 were haptenated in *ex vivo* human skin treated with bromobimanes (Bauer et al., 2011; Simonsson et al., 2011). Other epidermal keratin pairs (e.g. suprabasal epidermal pair K1/K10) were not haptenated. Another study, utilising HR-MAS NMR found that methyldodecanosulfonate haptenated His, Met and Cys residues in reconstituted human epidermis (RHE), but mostly Lys residues in human serum albumin (HSA) (Elbayed et al., 2013). Similar studies showed chemoselectivity of α-methylene-γ-butyrolactone for His residues of RHE (Debeuckelaere et al., 2015) and demonstrated differences in nucleophile targeting of methylisothiazolinone (MI) and methylchloroisothiazolinone (MCI) (Debeuckelaere et al., 2016).

Identification of haptenation sites in a complex and dynamic proteome and quantification of the haptenated proteins remains challenging. We previously demonstrated the utility of combining a dual isotope labelling approach with data-independent acquisition mass spectrometry in a single protein and performed Top3 quantitation (Silva et al., 2006) in cell and tissue lysates (Parkinson et al., 2020, 2018; Parkinson et al., 2014). Despite high concentrations of potent sensitisers and prolonged incubation time in these studies, the levels of haptenation observed were low. Whilst the ability to detect a vanishingly low level of haptenation demonstrated the high sensitivity of the approach, the data did not provide insights on the dynamics of protein haptenation over time nor of the overall cellular response to sensitiser treatment.

The study presented here utilises the same sensitive combination of stable isotope labelling and data-independent acquisition mass spectrometry with the addition of Top3 quantification (Silva et al., 2006) and SuperSILAC (Geiger et al., 2010) to accurately quantify changes over a 48 h time course in the proteome of HaCaT cells exposed to a subtoxic concentration of the potent sensitiser 2,4-dinitro -1-chlorobenzene (DNCB) for 4 h. Previous observations linking protein abundance as a determinant of protein haptenation are confirmed and the degree of specificity in haptenation of certain proteins further explored. We observe the dynamics of haptenation in living cells which point to additional factors which may influence the overall level of protein haptenation.

2. Materials and methods

2.1. Cell culture of skin cell lines

The human squamous carcinoma cell line A431 and the human malignant melanoma cell line A375 were purchased from ECACC. The human dermal fibroblast primary cell line HDFa was purchased from Life Technologies and the adherent keratinocyte cell line HaCaT was purchased from Cell Line Service GmbH (Eppelheim, Germany).

HaCaT and A431 cell lines were cultured in Dulbecco's Modified Eagle Medium (DMEM), high glucose, supplemented with 10 % heat inactivated fetal calf serum, 2 mM L-glutamine, 100U/mL Penicillin and 100ug/mL Streptomycin, at 37 °C and 5 % CO_2. A375 were cultured in DMEM, high glucose, supplemented with 15 % heat inactivated fetal calf serum, 2 mM L-glutamine, 100U/mL Penicillin and 100ug/mL Streptomycin), at 37 °C and 5 % CO_2. HDFa were cultured in A375 cell line complete media, with the addition of 1 % Non-essential amino acids (NEAA). Once the cells had reached approximately 80 % confluency, they were sub-cultured by detaching the cells from the surface of the culture flask with 0.25 % Trypsin-EDTA (Life Technologies). Cells were reseeded into fresh culture flasks at the following seeding densities: HaCaT at 1×10^4 cells/cm^2; A431 at $2-4 \times 10^4$ cells/cm^2; A375 at $1-3 \times 10^4$ cells/cm^2; and HDFa at 5×10^3 cells/cm^2.

2.2. Preparation of SILAC labelled skin cell reference

2.2.1. Cell growth and Stable isotope labelling of amino acids in cell culture (SILAC)

The skin cell reference standard was prepared by combining SILAC heavy labelled proteomes from HaCaT, A431, A375 and HDFa cell lines as follows. Each cell line was transferred to fresh culture flasks (once they had reached 70 % confluency) and cultured in SILAC DMEM medium (supplemented with dialyzed FCS and other components as needed for each cell line described above) where Lys and Arg had been replaced with $^{13}C_6^{14}N_2$-Lys and $^{13}C_6^{14}N_4$-Arg (Dundee Cell Products). The cells were cultured in order to achieve at least 8 population doublings, thus enabling the heavy lysine and arginine to be fully incorporated into the proteomes of the cells. The % of heavy label incorporation was estimated by harvesting a small aliquot of cells and analysing by GeLC-MS/MS as described below.

2.2.2. GeLC-MS/MS

Cells adhered to the surface of 1 x T75 flasks were washed twice with 6 mL of Hanks Buffered Saline Solution (HBSS) (Gibco, Life Technologies). Cells were trypsinised and the cell pellet lysed in 100 μL of lysis solution (25 μL LDS sample buffer, 10 μL of 0.5 M DTT and 65 μL of H_2O) at 70 °C for 10 min. The cell lysate was clarified by centrifugation at 13,000 x*g* for 10 min and 20 μL of the supernatant was loaded into 2 lanes of a 4–12 % Bis-Tris gel (Life Technologies) at 200 V for approximately 45 min. Following staining with Colloidal Coomasie Blue, gel tracks (7 cm length) were excised, cut into 25 equal-sized pieces and subjected to *in situ* trypsin digestion using the method of Shevchenko et al*(*Shevchenko et al., 1996*)*. The resulting peptides were analysed using nano-capillary liquid chromatography tandem mass spectrometry (LC–MS/MS) as described below.

2.2.3. Preparation of SuperSILAC skin cell reference

Once GeLC-MS/MS confirmed that each cell line had greater than 97 % incorporation of heavy isotope labels, the cells were kept in culture for a further 2 passages to achieve between 3×10^7 and 1×10^8 cells/mL. The cells were removed from the flask surface by incubating with Trypsin-EDTA for 5 min., then washed twice by suspending in 10 mL of HBSS and pelleting by centrifugation at 1200 rpm for 5 min. Harvested cells were lysed with the addition of 500 μL of lysis buffer (0.1 % SDS in 0.1 M TEAB) and sonicating at an amplitude of 2–3 for 30 s with 30 s rest, repeated 5 times, on ice. (Q500, Fisher Scientific)

The protein concentrations of the lysates were measured using a Direct Detect Infra-Red (IR) Spectrometer (Millipore). Equal concentrations of each cell line lysate were combined to make a 1 mg/mL stock in lysis buffer, aliquoted and stored at −80 °C until required.

2.3. Treatment of HaCaT cell lines with DNCB and analysis by mass spectrometry

2.3.1. Sensitiser preparation

DNCB (CAS 97-00-7; 99 % purity; MW 202.55 Da) was obtained from Sigma, UK, and DNCB-D_3 (99 % purity; MW 205.57 Da) was obtained from QMX Laboratories.

A stock solution of DNCB was made as a 50:50 mix, by molar concentration, of un-labelled sensitiser and stable isotope labelled sensitiser in 100 % Ethanol and diluted with serum free and phenol red free DMEM/F12 media to a final working concentration of 10 μM DNCB and

0.2 % ethanol. This concentration has previously been determined as subcytotoxic *in vitro* (Jacquoilleot et al., 2015) and comparable to human DNCB sensitising concentrations (Friedmann, 2006), considering lack of epidermal barrier and lower cell density of *in vitro* experiments.

2.3.2. Sensitiser modification of a keratinocyte cell line

HaCaT cells in the growth phase were harvested and seeded into 13 culture dishes at 3×10^5 cells per culture dish. Once the cells had been left for two days to adhere and equilibrate, the media was aspirated from the plates and replaced with 3 mL of 10μM DNCB, or media only for the controls, and incubated at 37 °C and 5% CO_2. Cells from one untreated culture dish were harvested as described previously for 0 h control timepoint. Cells from one DNCB treated and one untreated culture dish were harvested after 1 h, 2 h and 4 h. Harvested cells were rinsed with sterile HBSS, as described previously and a small aliquot was taken for estimation of cell concentration via trypan blue staining, the remaining samples were pelleted and stored at −80 °C until they were lysed. All media was removed from the remaining culture plates and the cells were cultured further in fresh serum free, phenol red free DMEM/F12 media. Cells were harvested from these plates at 8, 24 and 48 h from the start of the experiment (or 4, 20 and 44 h after the test chemicals were removed) (Fig. 1).

2.3.3. Cell lysis and spike-in SuperSILAC skin reference standard

Cell pellets stored at −80 °C were thawed on ice and sonicated as described above in 150 μL of cell lysis buffer and protein concentration determined using IR Spectroscopy. To each 50 μg of sensitiser treated (or control) cell lysate, an equal concentration (50 μg) of heavy labelled SuperSILAC standard was added, and the final volume made up to 100 μL in lysis buffer.

2.3.4. Protein digestion and peptide fractionation

To 100 μg of protein lysate, 4 volumes of methanol was added, the sample vortexed, before adding 1 vol of chloroform, vortexing again, and finally adding 3 volumes of water followed by a final vortex. The sample was centrifuged at 20,000 x g for 1 min, focusing the proteins between the organic and inorganic phases. The aqueous phase was removed, and 4 volumes of methanol added, followed by a short vortex. The precipitate was pelleted by centrifuging at 20,000 x g for 2 min, the methanol was aspirated and the pellet dried under vacuum using a SpeedVac (adapted from (Wessel and Flugge, 1984)). The pellet was re-solubilised in 100 μL buffer containing 6 M urea, 2 M thiourea and 10 mM Hepes, pH 7.5. Proteins were reduced with 1 mM DTT for 1 h at RT, alkylated with 5.5 mM IA for 45 min in the dark at room temperature, and then digested for 4 h with Lys-C (1/50 w/w). Peptides were then diluted four times with 20 mM ammonium bicarbonate and digested with sequencing grade modified trypsin (1/50 w/w) overnight at RT. After digestion the samples were spiked with 150 fmol of enolase and 150 fmol of *E. coli* digest standards (Waters, Manchester) to enable protein estimation by Hi3 calculation(Silva et al., 2006). The peptides were fractionated across Immobiline IPG strips, pH 3–10 using the Agilent 3100 OFFGEL Fractionator and fractions desalted using a C_{18} SPE 96 well plate (3 M, Minnesota) as described previously (Parkinson et al., 2020, 2018). Samples were lyophilised and stored at −20 °C.

2.3.5. Mass spectrometry analysis

Samples were resuspended in 0.1 % Formic Acid and approximately 1–2 μg of sample loaded onto a reverse phase trap column (Symmetry C18, 5 μm, 180 μm ×20 mm, Waters), at a trapping rate of 5 μL/min and washed for 10 min with buffer A prior to the analytical nano-LC separation using a C18 Reverse phase column (HSS T3, 1.8 μm, 200 mm ×75 μm, Waters Corporation, USA). Peptides were fractionated over a 90 min linear gradient from 1 % acetonitrile + 0.1 % formic acid up to 60 % acetonitrile + 0.1 % formic acid, at a flow rate of 300 nL/min. Eluted samples were sprayed directly into a Synapt G2-S mass spectrometer (Waters Corporation, Manchester, UK) operating in MS^E mode. Data was acquired from 50 to 2000 *m/z* using alternate low and high collision energy (CE) scans. Low CE was 5 V and elevated collision energy ramp from 15 to 40 V. Ion mobility was implemented prior to fragmentation using a wave height of 650 m/s and wave velocity of 40 V. The lock mass Glu-fibrinopeptide, $(M + 2\ H)^{+2}$, $m/z = 785.8426$) was infused at a concentration of 100 fmol/μl with a flow rate of 250 nl/min and

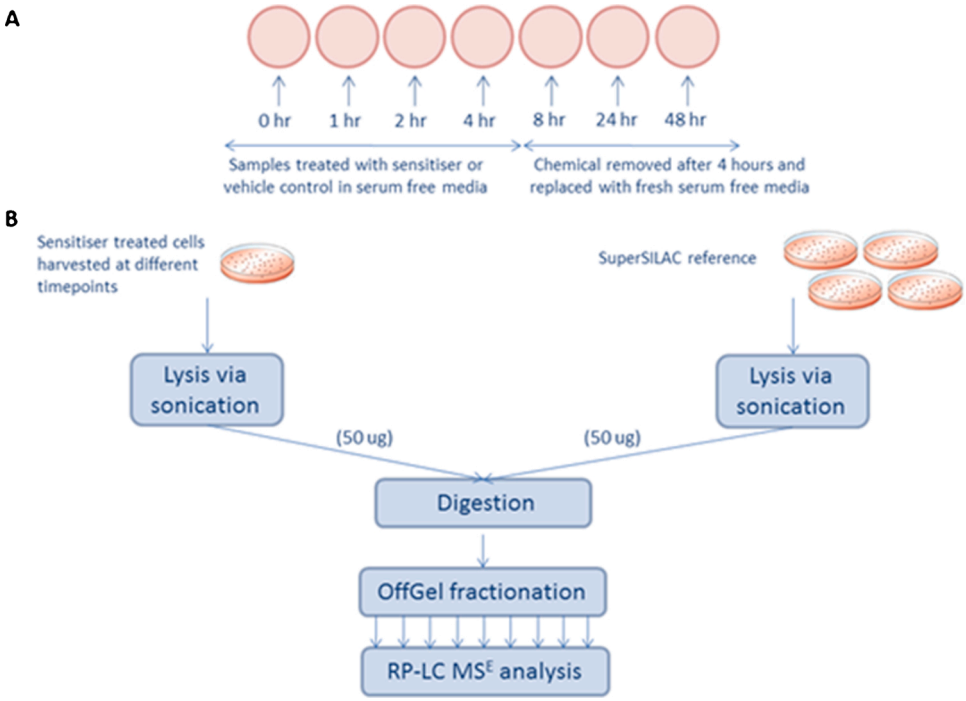

Fig. 1. Schematic of experimental setup. A: Cells are treated with sensitiser for 4 h, the sensitiser removed and the cells cultured for a further 44 h with cells being harvested at different timepoints; B: each sample is then lysed and 50 ug is mixed with 50 ug of the SuperSILAC reference mixture prior to digestion and fractionation for RP-LC MS^E analysis.

acquired every 60 s.

2.4. Database searches

The raw mass spectra were submitted to ProteinLynx Global Server executables (version 3.0.1 for Apex3D.exe and Peptide3D.exe; version 3.0.2 for MergeFractions.exe and IADBs.exe; Waters, Manchester, UK) using batch commands. The data was processed to generate reduced charge state and deisotoped precursor and associated product ion mass lists. These mass lists were then searched against the human UniProt protein *H. sapiens* sequence database. A maximum of two missed cleavages were allowed for tryptic digestion, the fixed modification was set to carboxyamidomethylation of Cys and the variable modifications were set to contain oxidation of Met; carbamylation of Lys and N-terminus; and DNP modification of Cys, Lys, Tyr, His and Arg; the fixed modifier group of SILAC $R_{10}K_8$ was also included. Precursor ion and product ion mass tolerances were automatically calculated. The false discovery rate (FDR) was estimated with decoy-fusion database searches and were filtered to 1% FDR. Modified peptides were confirmed by observing a unique 'signature' of 2 peptide isotope clusters with fixed $\Delta m/z$ in an MS spectrum and the exact location of haptenation confirmed by manual inspection of the product ion spectrum of the identified modified precursor. Following database searching, the data was filtered as previously described (Parkinson et al., 2018).

2.5. Statistical analysis

Absolute protein abundance of the Hi3 spectra was calculated based upon the Top3 method of Silva et al. (2006) (Silva et al., 2006), where the sum of the intensity of the 3 most abundant peptides of an enolase digest standard at a known concentration was used as a response factor to estimate the concentration of each protein in the samples based on the sum of the intensity of their 3 most intense peptide signals. The absolute protein abundance of each protein was used to estimate nucleophile content, as previously described (Parkinson et al., 2018).

Relative protein abundance of the superSILAC spectra was obtained by calculating the median of the ratios between light to heavy lysates for all quantified peptides in the protein (Itzhak et al., 2019). This led to the quantification of a total of 5544 proteins among all control samples and a total of 6259 proteins in the DNCB treated samples through the SILAC ratios.

Data analysis was performed using Perseus software (version 1.6.0.0) (Tyanova et al., 2016). Significant change in time-dependent protein abundance (absolute and relative) was calculated using a paired *t*-test between the control and DNCB treated sample for each time point. Permutation based FDR was set to 0.05; the s0 parameter was set to 0.1; number of performed randomizations was set to 250 with grouping of biological replicates preserved in randomization (Itzhak et al., 2019). Data were filtered for 66.7 % valid values before the test.

3. Results

Dual stable isotope labelling (Parkinson et al., 2020, 2018; Parkinson et al., 2014) was used to examine the details and dynamic of haptenation in living HaCaT cells over 48 h treated by a subtoxic concentration (10 μM (Jacquoilleot et al., 2015)) of the potent sensitiser DNCB for 4 h. Previous studies using this approach utilised either model proteins, keratinocyte or skin tissue lysates and artificially high, clinically irrelevant concentrations of sensitisers and served as method development studies establishing sensitivity of the approach to detect very low level of haptenation within complex proteomes. This study makes use of the sensitivity of the method to explore the haptenation in living cells at subtoxic sensitiser dose.

The current study identified a total of 7212 proteins from the HaCaT cell line of which 5721 proteins were in the control and 6461 proteins in the DNCB treated samples.

Significant change in time-dependent protein abundance was calculated using a paired *t*-test between the control and DNCB samples for each time point. The volcano plot comparing absolute protein abundances (Top3 spectra) showed no significant changes between the control and DNCB sample for each time point (Supplementary data 1, Adenine phosphoribosyltransferase represents a single outlier at t = 48 h). Similarly, when compared to the superSILAC reference standard, no significant changes were observed when relative protein abundances were compared between control and DNCB samples for each time point (Supplementary data 2). Together, the quantitative analyses indicate that treatment with a subcytotoxic concentration of DNCB for 4 h did not cause any significant changes in protein expression in living HaCaT cells over 48 h.

3.1. Protein modification

From a total of 6461 proteins (with two or more matched peptides) identified from the DNCB treated HaCaT cell line, 360 peptides (related to 308 proteins) were found modified by DNCB at one or more residues and within at least one time point (4.8 % of the HaCaT cell proteome) (Supplementary data 3).

A total of 556 distinct instances of DNCB haptenation were observed in the HaCaT proteome over 48 h (more than twice the number previously observed in HaCaT cell lysates). Of these we were able to confirm the amino acid site of haptenation for 215 and the identification of an additional 341 haptenated peptides, but where the exact location of the nucleophilic amino acid modified within the peptide could not be confirmed. Including all possible modified residues resulted in overestimation of the total number of modified residues. The highest total number of modifications was observed on Lys residues (161), followed by Tyr (108) and His (103), whereas Arg and Cys had 100 and 84 modifications, respectively. Without considering quantitative data, DNCB appears to show a higher preference towards amine type nucleophiles compared to thiol (Fig. 2).

Utilising protein quantitation data from 'Top3′ method, the number of copies of each protein per cell were calculated and total number of 'available' nucleophiles in the HaCaT proteome was derived as described previously (Parkinson et al., 2018). Comparison between 1−48 h shows that the overall percentage of each nucleophile remains constant throughout the experiment (Supplementary data 4). This is consistent with earlier observation of minimal overall proteome change in this study and data obtained from previous studies using HaCaT cell and human skin lysates, indicating that HaCaT proteomes are comparable in their nucleophilic 'make-up' between experiments. These values were used to calculate the percentage of modified nucleophiles observed at each time point.

The proportion of haptenated nucleophiles reaches a maximum of approximately 0.25 % of the total available nucleophiles at the 4 h time point after which the level of haptenation subsides considerably to barely detectable levels at 24 and 48 h (Fig. 3). Haptenation of Cys is dominant in the first 4 h of treatment, which contrasts with our conclusion made using a simple count of observed modifications. Equally, this is also in contrast to the conclusions of experiments using prolonged incubation of lysates with DNCB, where the highest level of haptenation was found on Lys residues. Notably, the actual quantity of haptenated protein versus the non-haptenated version cannot be calculated using this approach. This is a consequence of the likely change of ionisation efficiency of haptenated peptides in the ion source of the mass spectrometer compared to their non-haptenated counterparts. An assumption, therefore, had to be made that if a peptide was observed haptenated at a certain nucleophile, that all copies of the protein containing that peptide were haptenated at that nucleophile. As a result, the actual level of haptenation is overestimated.

Number and abundance of haptenated proteins over the 48 h time course varied considerably, with the 1 h and 2 h time points showing the highest number of observed DNCB modifications (Table1). After 4 h the

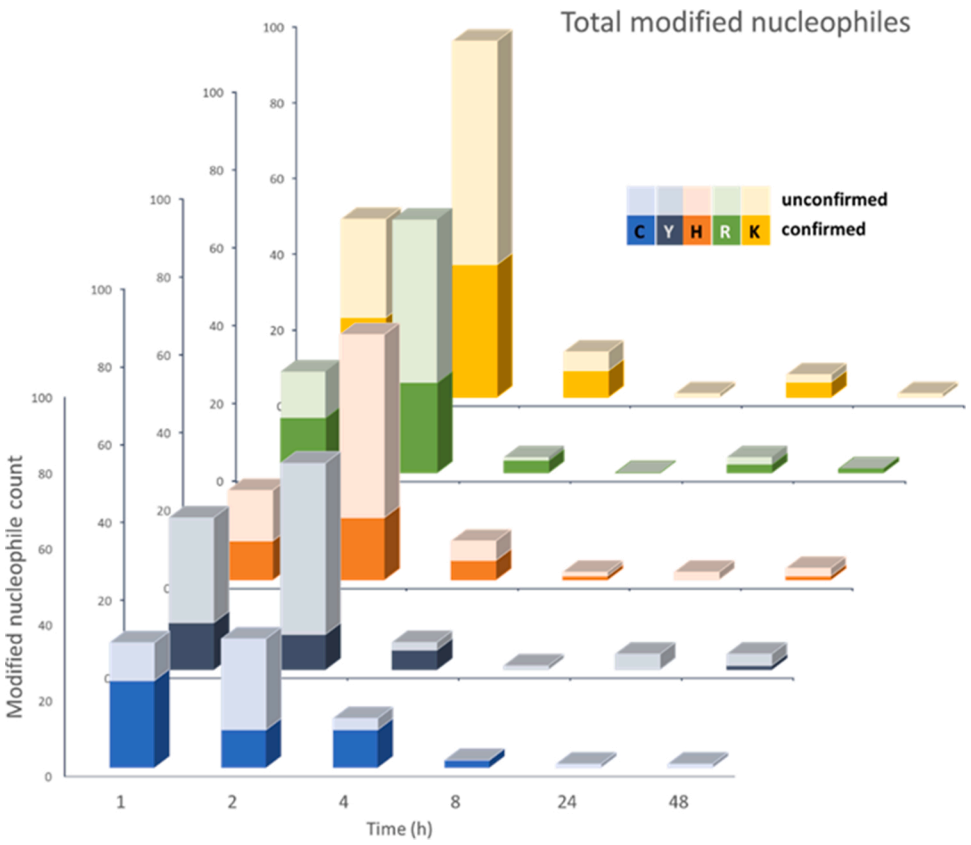

Fig. 2. Total count of all observed instances of haptenated residues in HaCaT cell lines treated with DNCB over 48 h. Solid colours – exact location of the haptenated residue was confirmed, faded colours – the modification(s) was observed by the presence of distinct isotopic signature, however, due to low quality fragmentation spectra, the exact location could not be unambiguously confirmed; the most likely location is suggested. C – cysteine; Y – tyrosine; H – histidine; R – arginine; K - lysine.

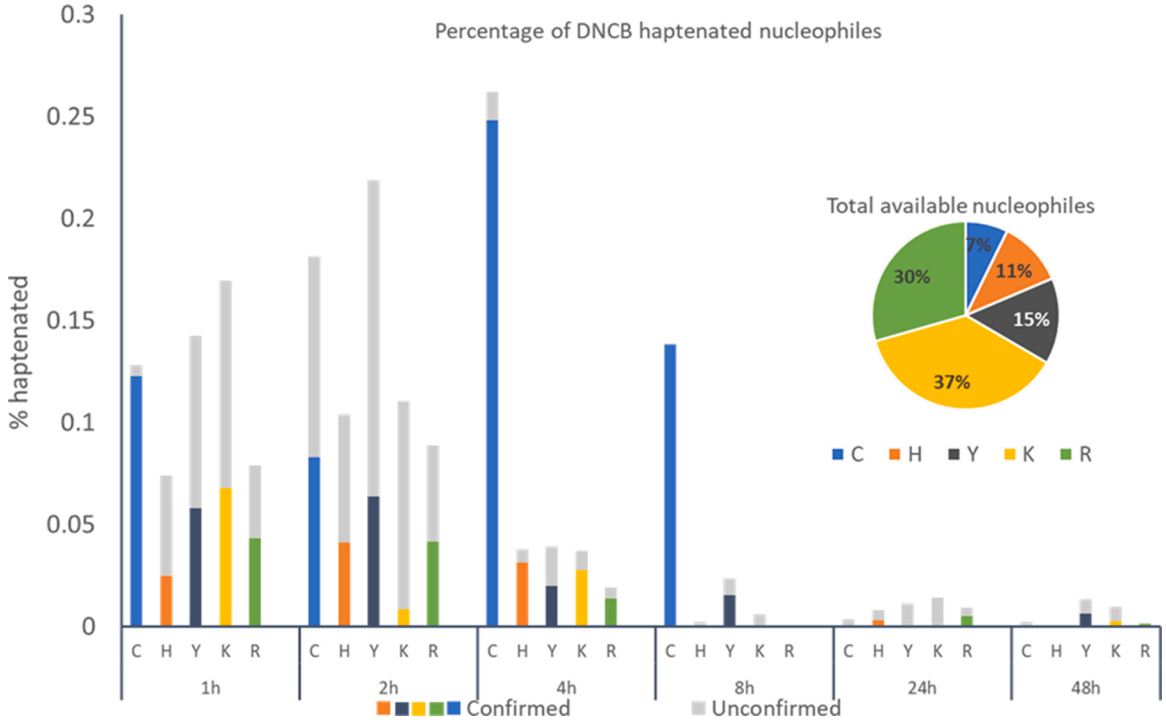

Fig. 3. The percentage of haptenated nucleophiles observed in the HaCaT cell line treated with DNCB over 48 h. Inset: proportion of total available nucleophiles in HaCaT proteome, calculated using the amount of each identified protein (fmol) and multiplying by Avogadro's constant to obtain the number of copies of each protein. The number of copies and the protein sequence are used to calculate the total number of available nucleophiles. The 'available' nucleophiles count does not consider a possibility that certain nucleophilic residues may not be accessible for modification by DNCB. However, this method is considered the best estimate, given that hydrophobic interactions play the major role in protein stability and folding which leaves charged and polar residues, that contain nucleophilic groups, mainly exposed to the protein surface (Lee and Vasmatzis, 1997). C – cysteine; Y – tyrosine; H – histidine; R – arginine; K - lysine.

Table 1
Total number of haptenated proteins and haptenation sites detected per time point (*includes all modifiable residues when more than a single modifiable residue is present in the peptide sequence).

Time (h)		1	2	4	8	24	48
Number of haptenated proteins		109	166	34	4	12	7
Number of DNCB modifications	Sites Confirmed	80	93	30	3	6	3
	Sites Unconfirmed*	88	216	16	3	11	7
	Total	168	309	46	6	17	10

cell media is changed and a considerable amount of haptenated proteins which are expelled from the cells are likely removed, which could explain the low number of haptenated proteins at 8 h, 24 h and 48 h.

Comparison between the proteins haptenated at different time points in relation to the Gene Ontology terms for cellular compartment revealed the presence of a wide range of compartments including extracellular space, cytoplasm, cytoskeleton, nucleus and mitochondrion (Supplementary data 5). Enrichment of proteins belonging to keratin filaments and the proteasome complex was noted at 8 h, 24 h and 48 h. Haptenated proteome contains components involved in regulatory processes, transport and metabolism (Supplementary data 6). Antigen processing and presentation, amino acid metabolism and cell death are enriched among haptenated proteins detected at 8 h, 24 h and 48 h. Thus, both cellular component and biological process GO term analyses agree with the nature of the experiment, however, a high enrichment of terms detected at later time points can be a consequence of a low number of modifications detected at these time points.

A considerable number of haptenation sites were observed on abundant proteins, particularly up to the 4 h time point (Fig.4). However, haptenation of low abundant proteins is observed throughout the time course, with numerous modifications observed on proteins with very low abundance, particularly at 1 h and 2 h. The distribution of abundance in the haptenated and non-haptenated set of proteins was compared per each time point. Haptenated proteins are marginally more abundant and this difference is statistically significant according to the Kolmogorov–Smirnov test (Supplementary data 7). The statistical analysis is less reliable at later time points (8−48 h) due to the lower number of haptenated proteins. Additionally, the quantity of haptenated proteins versus their non-haptenated versions could not be determined, therefore an assumption that all copies of the protein were haptenated at the same residue is likely an overestimation.

Approximately one fifth (21) of the top 100 highly abundant proteins were haptenated by DNCB. Of those, certain keratin pairs are most prominent. Keratins are cytoplasmic intermediate filament proteins expressed by epidermal (and other epithelial) cells forming a complex cytoskeletal network from heterodynamic pairs, which are assembled in a 1:1 M ratio of matching type I and type II keratins. DNCB modifications were found on the highly abundant K5/14 pair (P13647 and P02533, respectively), expressed in active basal human epidermis (Alam et al., 2011) as well as the highly abundant K6/K16-17 pair (expressed in keratinocytes of injured skin (Zhang et al., 2019)).

Other highly abundant haptenated proteins include actin (P60709, another key part of the cytoskeleton), heat shock cognate 71 kDa protein (P11142, plays pivotal role in protein quality control system), 60 kDa mitochondrial heat shock protein (P10809, key to protein folding), prelamin A/C (P02545, component of nuclear lamina), heat shock

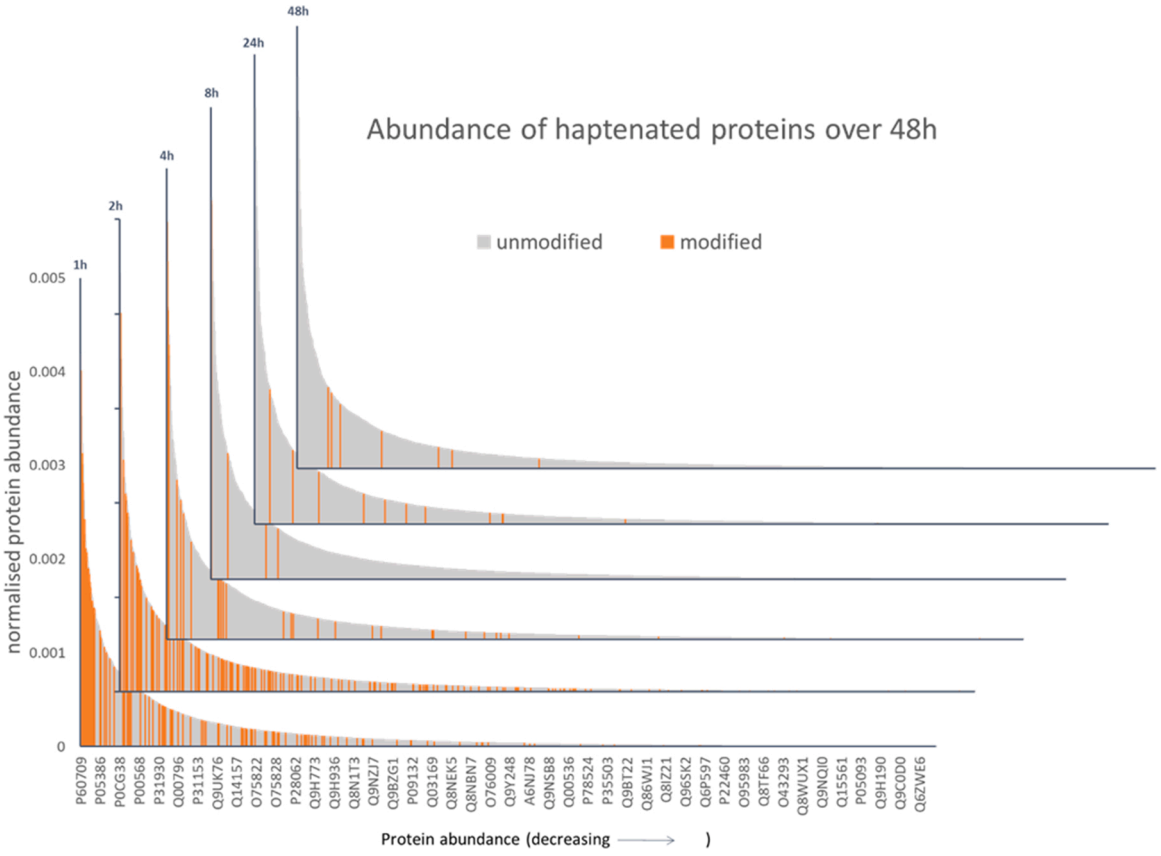

Fig. 4. Abundance of haptenated proteins in HaCaT cell line treated with DNCB (orange bars) versus the abundance of all quantified HaCaT proteins (light grey bars). Due to likely differences in ionisation efficiency between haptenated peptides and their non-haptenated counterparts, the quantitative data on the proportion of each protein that was haptenated could not be obtained. An assumed 100 % haptenation (the height of orange bars) was used here to illustrate the possible influence of protein abundance on the likelihood of haptenation occurring. The data demonstrates that high abundance of protein plays a role in the level of haptenation, however that there are possibly multiple factors governing haptenation, resulting in modification of medium and low abundant proteins.

protein beta-1 (P04792, molecular chaperone, involved in protein maintenance), peroxiredoxin-1 (Q06830, involved in peroxide detoxification), malate dehydrogenase (P40926), myosin-9 (P35579, plays a role in cytokinesis), glucose-6-phosphate isomerase (P06744, catalyses the second step in glycolysis and reverse reaction in gluconeogenesis), mitochondrial ATP synthase subunit alpha (P25705, cell energetics, produces ATP from ADP) and protein disulphide isomerase (P07237, catalyses formation, breakage and rearrangement of disulphide bonds).

However, 79 of the top 100 highly abundant proteins were not haptenated by DNCB including vimentin (P08670), l-lactate dehydrogenase A chain (P00338), Annexin A2 (P07355), histone H4 (P62805), tubulin beta chain (P07347), pyruvate kinase PKM (P14618), beta-actin-like protein (Q562R1). Most notably, not all highly abundant keratins were haptenated. For example, the K1/K10 pair (P04264 and P13645, respectively), expressed in suprabasal differentiated epidermis, were not haptenated, likely due to their Cys residues involvement in disulphide bridges (unlike K5/K14 pair, expressed in basal epidermis and more likely to have free Cys) (Simonsson et al., 2011). Similarly, K8/K19 pair (P05787 and P08727, respectively), primary keratins of simple epithelia also found in some stratified epithelia, like skin (Bragulla and Homberger, 2009; Moll et al., 2008) were also highly abundant, but not modified by DNCB.

Haptenation sites were confidently determined for numerous low abundant proteins, more prevalent at early time points (Supplementary data 3). It is unclear what is driving the haptenation of these low abundant proteins, but the specific microenvironment of target residues could provide the explanation. Slight differences in the microenvironment of a target residue can be probed by measuring or calculating the pKa value from a given protein structure (Georgescu et al., 2002). In highly polar or polarizable microenvironments, the charged form of an ionizable group will predominate; in less polar or polarizable microenvironments, the neutral form will be favoured and the pKa value will be shifted relative to the value observed in water (Harms et al., 2009). The pKa values were calculated for all confidently determined haptenation sites with available protein structures (from Protein Data Bank (Burley et al., 2018)) (Supplementary data 8). The pKa calculations showed no statistically significant changes between pKa values of the haptenated and non-haptenated nucleophiles (Arg, Lys, Cys, His and Tyr) (p-value >0.05, two sample Kolmogorov-Smirnov test). Importantly, calculation of pKa values does not accurately reproduce the experimental measurements due to the absence of protein dynamics in the calculations (Nielsen et al., 2011) and this affects the obtained results when a very limited number of sites is considered.

Several instances of haptenated residues buried deep inside the protein structure were observed, whilst other freely available and exposed nucleophilic residues were not haptenated. For example, Annexin A3 (P12429), Protein disulphide-isomerase (P07237) and Ski-like protein (P12757) were haptenated at Arg 274, His 256 and Cys 218, respectively (Fig. 5). The side chains of all three residues are located deep inside the protein and are only partially accessible to ligands. In fact, in 29 proteins (41.4 %) of the total 70 proteins with 3D structure available, side chains of the haptenated residue were not fully accessible to solvent (Supplementary data 3, % of buried side chain > 0 %). This observation implies that the microenvironment of haptenated residues plays a role in specificity for the haptenation site. Such microenvironments are not simply defined by the pKa value of the target nucleophile, but rather with the hapten-compatible van der Waals surface and charges that facilitate induced fit between the two molecules. Furthermore, this is difficult to validate using molecular docking software which lacks the ability to account for covalent bonding between molecules (Pagadala et al., 2017).

A total of 63 different proteins had more than one DNCB modification either at a single or multiple time points (Supplementary data 9). Multiple modifications were observed throughout the time course apart from 8 h time point, with higher frequency at 1 and 2 h. The highest number of modifications on a single protein was 4, observed for P02538 (K6, type II cytoskeletal keratin, modified at Cys50, Cys76, Tyr216 and Cys473) followed by 3 modifications observed for P02533 (K14, type I cytoskeletal keratin, modified at Cys18, Cys40 and Arg446) and P13647 (K5, type II cytoskeletal keratin, modified at Cys55, Tyr222 and Cys479).

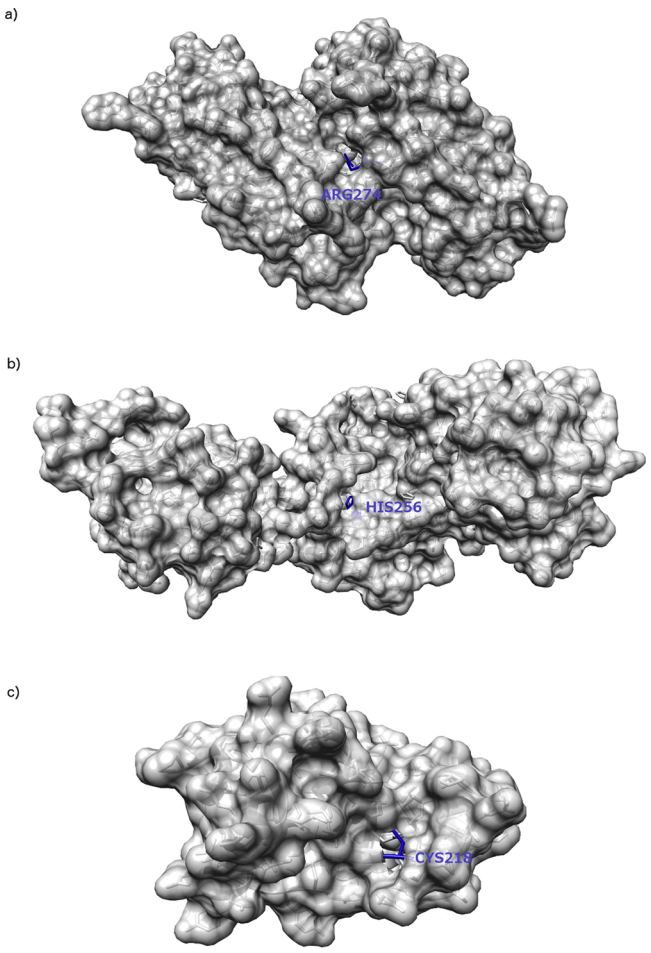

Fig. 5. Examples of haptenated residues with side chains are buried deep inside proteins. a) Arg 274 of Annexin A3 (P12429, 97 % buried); b) His 256 of Protein disulphide-isomerase (P07237, 70 % buried); c) Cys 218 of Ski-like protein in its reduced form (P12757, 47 % buried). Haptenated residues are shown in blue. (For interpretation of the references to colour in this figure legend, the reader is referred to the web version of this article).

Several low abundant proteins had multiple modifications (e.g. peptidyl-prolyl cis-trans isomerase FKBP8 (Q14318), ribosomal protein S6 kinase alpha-5 (O75582, involved in the regulation of inflammatory genes), K6C (P48668, keratin type II 6C, paired with K16-17 involved in wounding response), mitochondrial import inner membrane translocase subunit Tim10 B (Q9Y5J6), protein ecdysoneless homolog (O95905, regulator of p53/TP53 stability and function).

The overlap of haptenomes (subsets of proteome haptenated by DNCB) over time was minimal, although several instances of proteins haptenated at more than one time point were observed (single or multiple sites) (Supplementary data 10). These are rarely observed for more than 2 time points, with only 1 exception (K5 keratin) and occur exclusively for highly abundant proteins.

4. Discussion

Haptenation of skin proteins, a key MIE in skin sensitisation is routinely exploited to rationalise the ability of a chemical to sensitise an individual and confirmed/measured experimentally to provide data for

risk assessment. Our knowledge of the dynamics of this process in human skin and understanding of the metrics required to improve determination of sensitiser potency is lacking. Previous studies utilising a dual isotope labelling approach provided an important bridge between using simple nucleophilic models and single model proteins and gaining useful information about more realistic and physiologically relevant levels and specificity of haptenation. Having demonstrated the applicability of the dual stable isotope labelling approach to detect low level haptenation in complex mixtures of proteins and addressed the challenge of method sensitivity, we have taken the opportunity to investigate haptenation in a relevant living cell model over time at a subtoxic concentration to provide insights into the dynamics of haptenation.

To assess the coverage of the identified proteome of living HaCaT cells, we have compared it to the proteome of our previous study where cell lysates were incubated with high concentration of DNCB over a prolonged time (a total of 6704 identified proteins) (Parkinson et al., 2018). An overlap of 69.2 % was observed across the two proteomes (4638 proteins in common). This medium level of agreement is likely attributed to the ability to detect greater numbers of low abundant proteins from two different samples and at different time points. The identified proteome from the current study was also compared to the study where HaCaT cells were exposed to arsenic over prolonged time (total of 2147 identified proteins) (Mir et al., 2017). The higher overlap (2021 proteins in common (94.1 %)) probably reflects the lower sensitivity of experiments and detection of relatively highly abundant proteins by Mir and colleagues (Mir et al., 2017).

The minimal change observed in differential expression of the proteome matches expectation that, at a sub-toxic dose, the cells react by employing powerful defence mechanisms to minimise the potentially detrimental effect of haptenation. It is reasonable to assume that if the capacity of a cell to remove the electrophile has not been exceeded, no major changes to proteome should be observed.

Our current assessment of the extent of DNCB haptenation in living HaCaT cells corresponds with our previous high DNCB concentration long incubation analyses (Parkinson et al., 2018) in which 210 peptides (related to 162 proteins) were found modified by DNCB. However, only 28 haptenated proteins were found in common between both datasets with only one distinct DNCB haptenation event present in both (Cys 489 of Keratin, type II cytoskeletal 2 epidermal, P35908).

We observed considerable differences between the number of instances of haptenation of various nucleophiles (simply counting different nucleophiles modified) and the level of haptenation observed when quantitative data was taken into consideration. Based upon a simple count of the nucleophilic residue modified by DNCB, a preference for the amine type nucleophiles was noted. However, despite the obvious overestimation of the level of haptenation (assuming 100 % haptenation of the modified protein), a definite preference for thiols was observed in the second case, certainly up to 8 h. Notably, the 'available' nucleophiles count excludes the likelihood of nucleophiles not being accessible or situated in a microenvironment not conducive to haptenation. However, this method is considered the best estimate, as hydrophobic interactions play the major role in protein stability and folding which leaves charged and polar residues, that contain nucleophilic groups, mainly exposed on the surface (Lee and Vasmatzis, 1997). Understanding the nucleophilic make-up of skin and how an electrophilic chemical reacts with nucleophiles in these circumstances may help interpret the routinely measured reactivity of chemicals in *in chemico* assays and improve our ability to predict thresholds in sensitisation.

The rationale for the haptenation of certain proteins is certainly their high abundance. In particular specific keratin pairs (found in basal layers of epidermis in human skin and previously seen modified by others (Bauer et al., 2011; Simonsson et al., 2011)) are modified, often at more than one residue and sometimes at more than a single time point. However, several other keratin pairs (typically found at upper layers of epidermis in skin) were equally abundant but were not modified. Keratin heterodimers of basal epidermis have Cys residues available, whereas in upper layers of epidermis keratin heterodimers are tightly packed and their Cys residues are involved in disulphide bridges, making them unavailable for haptenation. Additionally, most highly abundant proteins are not haptenated.

A previous study utilising human K14 as a model protein (Aleksic et al., 2008) without its natural pair K5, found DNCB haptenated several nucleophilic residues after prolonged incubation with a large excess of hapten (Cys40 (also seen haptenated in this study), Tyr46, Tyr129, Lys132, Tyr150, Lys203, Tyr204, Lys363 and Tyr415). Human cofilin, also used as a model protein by Aleksic et al. (Aleksic et al., 2008), was relatively abundant in the current study but was not haptenated by DNCB. A study using *ex vivo* human skin found C54 of K5 modified by monobromobimane (Bauer et al., 2011; Simonsson et al. 2011).The same residue (actually found to be C55 in human K5 sequence) was found modified by DNCB in this study.

Rationalising haptenation of low abundant proteins is more complex. Certain proteins were found modified at specific buried residues despite other nucleophiles being available and more accessible. Without further detailed investigation, it is unclear which specific conditions are responsible for haptenation of these residues. Whilst influence of neighbouring residues and microenvironment on the target nucleophile pKa may be an explanation for some specific proteins, no global shift in pKa could be reliably observed globally for haptenated nucleophiles. A possible explanation may emerge from understanding steric influences/hindrance and potentially protein-protein interactions which could considerably change the microenvironment for some affected nucleophiles.

Notably, the change of media at 4 h is a likely contributor to a considerable drop in observed level of haptenation at 8−48 h time points. Additionally, doubling the amount of cells at 48 h and thus reducing the chance of detection is another likely reason for lower detection at 48 h. Lack of full quantitation of the proportion of haptenated protein versus their non-haptenated counterparts results in almost certain overestimation of the overall level of haptenation.

Whilst abundance of certain proteins may be the key factor determining the level of modification, the haptenation cannot be described as a 'random' event. Clear 'rules' cannot be established for haptenation in a global proteome sense. It is possible, however, that haptenation of certain subsets of proteins is driven by their specific function and therefore determined by their structure and target nucleophile position, particularly in relation to interaction with other proteins. For those groups of proteins haptenation may be constrained by more than one factor. Further detailed quantitative investigation, specifically determination of the level of haptenation of individual proteins (versus their unmodified copies) as well as understanding microenvironment of target nucleophiles in 3D structure and protein-protein interactions would aid in determining these factors.

Despite the detailed study of haptenation dynamics, our analyses do not show all the elements of the cellular response to an external electrophilic insult, in particular the changes in the levels of small molecular nucleophiles, namely thiols (such as GSH). Electrophiles which react via S_N2, S_NAr or Michael addition reaction with nucleophiles would react with GSH concomitantly and likely faster, given the presence of glutathione-s-transferases (GSTs, several isoforms were detected in this study). For example, 10μM DNCB depletes over 50 % of GSH in HaCaT cells within 1 h and the level of GSH recovers to baseline by 24 h (Jacquoilleot et al., 2015). Efforts to understand how the cells deal with external electrophilic insult would be aided by the inclusion of measurements of additional concomitant reactivity driven events. In addition to this, consideration should also be given to concomitant events resulting from disturbance of the redox balance upon exposure to an external electrophile. Lipid peroxidation triggered by an increase in ROS leads to production of additional endogenous electrophiles (mostly dicarbonyls and α,β-unsaturated aldehydes) which also covalently modify proteins (Pamplona, 2011). The influence of these events on

haptenation have not yet been investigated.

Following our baseline studies of haptenation in cell lysates, we concluded that applying the same approach over a shorter time in living cells would result in a lower level of haptenation, which was likely to be a subset of modifications observed in lysates. However, we found a comparable level of haptenation with almost no overlap between the two datasets (a single instance of a residue on a highly abundant protein was modified in both datasets). This, in addition to the observation that modification of the same proteins over the time course in this dataset are rare and only visible for a couple of highly abundant keratins, may indicate that haptenation is a reversible event. Evidence exists for instability and reversibility of covalent modifications in some instances (Kumagai and Abiko, 2017; Randall et al., 2013) and the contribution of selective electrophilic modification of proteins to redox signalling events (Long and Aye, 2016; Long et al., 2019). Alternative explanations are that additional haptenation over time may alter the protein digestion during sample preparation; or that haptenated peptides are further modified by processes such as oxidation, changing the m/z of the haptenated peptide, both of which would reduce the signal intensity of already observed modified peptides which are then below the threshold of detection at later time points.

DNCB was previously shown to activate the Nrf2 pathway at 10μM in HaCaT cells (Emter et al., 2010; Jacquoilleot et al., 2015) and it is therefore expected that DNCB haptenates human Kelch-like ECH-associated protein 1 (Keap1). Interestingly, Keap1 was detected in this study at a very low level which could not be quantified and no DNCB modifications were detected. It is possible that Keap1 modification occurs very early upon exposure to an electrophile, however Nrf2 activation has been reported at 2 h previously (Jacquoilleot et al., 2015). Several previously reported 'electrophile sensitive' proteins have been detected here. For example, highly abundant and haptenated by DNCB in this study, 60 kDa mitochondrial heat shock protein (P10809) and heat shock cognate 71 kDa protein (P11142) were previously reported as electrophile targets (Wong and Liebler, 2008). Thioredoxin was detected and highly abundant in HaCaT cells in this study, but was not haptenated by DNCB, despite previously being reported as a target (Wong and Liebler, 2008). Similarly, several low abundant aldehyde dehydrogenase isoforms were detected, previously reported as electrophile targets (Wall et al., 2014) but these also were not haptenated by DNCB. Other reported 'electrophile sensitive' proteins (IKKβ, LKB1-STKK, AP-1, H-Ras and PPARγ (Wall et al., 2014)) were not detected.

The present study offers insights into the complex events surrounding haptenation by DNCB in HaCaT cells upon subtoxic exposure. DNCB reacts via a single electrophilic mechanism (S_NAr) and whilst it is a potent sensitiser and a promiscuous hapten, the events observed here represent a single facet of electrophilic reactivity that can lead to sensitisation. Further studies of sensitisers reacting via different chemical mechanisms and less promiscuously should help to better define global dynamics of haptenation and multiple rules governing the key MIE in sensitisation. It is prudent to consider haptenation in mechanistic terms in conjunction with other (reactivity) related events in the cells which are exposed to reactive chemicals.

Funding information

This work was supported by Safety and Environmental Assurance Centre (SEAC), Unilever, UK.

Declaration of Competing Interest

None.

Acknowledgements

Instrumentation in the Centre for Proteomic Research is supported by the BBSRC (BM/M012387/1) and the Wessex Medical Trust. This work was funded as part of Unilever's on-going support in developing novel ways of delivering consumer safety.

Appendix A. Supplementary data

Supplementary material related to this article can be found, in the online version, at doi:https://doi.org/10.1016/j.tox.2020.152603.

References

Alam, H., Sehgal, L., Kundu, S.T., Dalal, S.N., Vaidya, M.M., 2011. Novel function of keratins 5 and 14 in proliferation and differentiation of stratified epithelial cells. Mol. Biol. Cell 22 (21), 4068–4078.

Aleksic, M., Pease, C.K., Basketter, D.A., Panico, M., Morris, H.R., Dell, A., 2007. Investigating protein haptenation mechanisms of skin sensitisers using human serum albumin as a model protein. Toxicol. In Vitro 21, 723–733.

Aleksic, M., Pease, C.K., Basketter, D.A., Panico, M., Morris, H.R., Dell, A., 2008. Mass spectrometric identification of covalent adducts of the skin allergen 2,4-dinitro-1-chlorobenzene and model skin proteins. Toxicol. In Vitro 22 (5), 1169–1176.

Aleksic, M., Thain, E., Roger, D., Saib, O., Davies, M., Li, J., Aptula, A., Zazzeroni, R., 2009. Reactivity profiling: covalent modification of single nucleophile peptides for skin sensitization risk assessment. Toxicol. Sci. 108 (2), 401–411.

Alinaghi, F., Bennike, N.H., Egeberg, A., Thyssen, J.P., Johansen, J.D., 2019. Prevalence of contact allergy in the general population: a systematic review and meta-analysis. Contact Derm. 80 (2), 77–85.

Alvarez-Sanchez, R., Basketter, D.A., Pease, C., Lepoittevin, J.P., 2004. Covalent binding of the 13c-labeled skin sensitizers 5-chloro-2-methylisothiazol-3-one (mci) and 2-methylisothiazol-3-one (mi) to a model peptide and glutathione. Bioorg. Med. Chem. Lett. 14 (2), 365–368.

Baltazar, M.T., Cable, S., Carmichael, P.L., Cubberley, R., Cull, T.A., Delagrange, M., Dent, M.P., Hatherell, S., Houghton, J., Kukic, P., et al., 2020. A next generation risk assessment case study for coumarin in cosmetic products. Toxicol. Sci.

Basketter, D.A., Gerberick, G.F., Kimber, I., 2001. Measurement of allergenic potency using the local lymph node assay. Trends Pharmacol. Sci. 22 (6), 264–265.

Bauer, B., Andersson, S.I., Stenfeldt, A.L., Simonsson, C., Bergstroom, J., Ericson, M.B., Jonsson, C.A., Broo, K.S., 2011. Modification and expulsion of keratins by human epidermal keratinocytes upon hapten exposure in vitro. Chem. Res. Toxicol. 24 (5), 737–743.

Bragulla, H.H., Homberger, D.G., 2009. Structure and functions of keratin proteins in simple, stratified, keratinized and cornified epithelia. J. Anat. 214 (4), 516–559.

Buehler, E.V., 1965. Delayed contact hypersensitivity in the guinea pig. Arch. Dermatol. 91, 171–177.

Burley, S.K., Berman, H.M., Bhikadiya, C., Bi, C., Chen, L., Di Costanzo, L., Christie, C., Dalenberg, K., Duarte, J.M., Dutta, S., et al., 2018. Rcsb protein data bank: biological macromolecular structures enabling research and education in fundamental biology, biomedicine, biotechnology and energy. Nucleic Acids Res. 47 (D1), D464–D474.

Chipinda, I., Ajibola, R.O., Morakinyo, M.K., Ruwona, T.B., Simoyi, R.H., Siegel, P.D., 2010. Rapid and simple kinetics screening assay for electrophilic dermal sensitizers using nitrobenzenethiol. Chem. Res. Toxicol. 23 (5), 918–925.

Chipinda, I., Mbiya, W., Adigun, R.A., Morakinyo, M.K., Law, B.F., Simoyi, R.H., Siegel, P.D., 2014. Pyridoxylamine reactivity kinetics as an amine based nucleophile for screening electrophilic dermal sensitizers. Toxicology 315, 102–109.

Chittiboyina, A.G., Avonto, C., Rua, D., Khan, I.A., 2015. Alternative testing methods for skin sensitization: nmr spectroscopy for probing the reactivity and classification of potential skin sensitizers. Chem. Res. Toxicol. 28 (9), 1704–1714.

Debeuckelaere, C., Berl, V., Elbayed, K., Moussallieh, F.M., Namer, I.J., Lepoittevin, J.P., 2015. Matrix effect of human reconstructed epidermis on the chemoselectivity of a skin sensitizing alpha-methylene-gamma-butyrolactone: consequences for the development of in chemico alternative methods. Chem. Res. Toxicol. 28 (11), 2192–2198.

Debeuckelaere, C., Moussallieh, F.M., Elbayed, K., Namer, I.J., Berl, V., Gimenez-Arnau, E., Lepoittevin, J.P., 2016. In situ chemical behaviour of methylisothiazolinone (mi) and methylchloroisothiazolinone (mci) in reconstructed human epidermis: a new approach to the cross-reactivity issue. Contact Derm. 74 (3), 159–167.

Dent, M., Amaral, R.T., Da Silva, P.A., Ansell, J., Boisleve, F., Hatao, M., Hirose, A., Kasai, Y., Kern, P., Kreiling, R., et al., 2018. Principles underpinning the use of new methodologies in the risk assessment of cosmetic ingredients. Comput. Toxicol. 7, 20–26.

Elbayed, K., Berl, V., Debeuckelaere, C., Moussallieh, F.M., Piotto, M., Namer, I.J., Lepoittevin, J.P., 2013. Hr-mas nmr spectroscopy of reconstructed human epidermis: potential for the in situ investigation of the chemical interactions between skin allergens and nucleophilic amino acids. Chem. Res. Toxicol. 26 (1), 136–145.

Emter, R., Ellis, G., Natsch, A., 2010. Performance of a novel keratinocyte-based reporter cell line to screen skin sensitizers in vitro. Toxicol. Appl. Pharmacol. 245 (3), 281–290.

Friedmann, P.S., 2006. Contact sensitisation and allergic contact dermatitis: immunobiological mechanisms. Toxicol. Lett. 162 (1), 49–54.

Geiger, T., Cox, J., Ostasiewicz, P., Wisniewski, J.R., Mann, M., 2010. Super-silac mix for quantitative proteomics of human tumor tissue. Nat. Methods 7 (5), 383–385.

Georgescu, R., Alexov, E., Gunner, M., 2002. Combining conformational flexibility and continuum electrostatics for calculating pkas in proteins. Biophys. J. 83 (4), 1731–1748.

Gerberick, G.F., Vassallo, J.D., Bailey, R.E., Chaney, J.G., Morrall, S.W., Lepoittevin, J.P., 2004. Development of a peptide reactivity assay for screening contact allergens. Toxicol. Sci. 81 (2), 332–343.
Gerberick, G.F., Vassallo, J.D., Foertsch, L.M., Price, B.B., Chaney, J.G., Lepoittevin, J.P., 2007. Quantification of chemical peptide reactivity for screening contact allergens: a classification tree model approach. Toxicol. Sci. 97 (2), 417–427.
Harms, M., Castañeda, C., Schlessman, J., Sue, G., Isom, D., Cannon, B., García-Moreno, B., 2009. The pka values of acidic and basic residues buried at the same internal location in a protein are governed by different factors. J. Mol. Biol. 389 (1), 34–47.
Henriot, S., Lepoittevin, J.P., Trifilieff, E., 2001. Haptenization of ovalbumin with the skin sensitizer methyl octanesulfonate: characterization of the methylated ova323-339 t-cell epitope at his331. J. Pept. Sci. 7 (6), 331–337.
Itzhak, D.N., Sacco, F., Nagaraj, N., Tyanova, S., Mann, M., Murgia, M., 2019. Silac-based quantitative proteomics using mass spectrometry quantifies endoplasmic reticulum stress in whole hela cells. Dis. Model. Mech. 12 (11).
Jacquoilleot, S., Sheffield, D., Olayanju, A., Sison-Young, R., Kitteringham, N.R., Naisbitt, D.J., Aleksic, M., 2015. Glutathione metabolism in the hacat cell line as a model for the detoxification of the model sensitisers 2,4-dinitrohalobenzenes in human skin. Toxicol. Lett. 237 (1), 11–20.
Kimber, I., Dearman, R.J., Basketter, D.A., Ryan, C.A., Gerberick, G.F., 2002. The local lymph node assay: past, present and future. Contact Derm. 47, 315–328.
Kumagai, Y., Abiko, Y., 2017. Environmental electrophiles: protein adducts, modulation of redox signaling, and interaction with persulfides/polysulfides. Chem. Res. Toxicol. 30 (1), 203–219.
Lee, B., Vasmatzis, G., 1997. Stabilization of protein structures. Curr. Opin. Biotechnol. 8 (4), 423–428.
Lepoittevin, J.P., 2006. The chemistry of skin allergy. ALTEX 23 (Suppl), 234–238.
Long, M.J.C., Aye, Y., 2016. The die is cast: precision electrophilic modifications contribute to cellular decision making. Chem. Res. Toxicol. 29 (10), 1575–1582.
Long, M.J.C., Wang, L., Aye, Y., 2019. Getting the right grip? How understanding electrophile selectivity profiles could illuminate our understanding of redox signaling. Antioxid. Redox Signal.
Luijten, M., Rorije, E., Sprong, R.C., van der Ven, L.T.M., 2020. Practical application of next generation risk assessment of chemicals for human health. Chem. Res. Toxicol. 33 (3), 693–694.
Magnusson, B., Kligman, A.M., 1970. Allergic Contact Dermatitis in the Guinea Pig. Identification of Contact Allergens. Charles C. Thomas, Springfield, Illinois.
Mir, S.A., Pinto, S.M., Paul, S., Raja, R., Nanjappa, V., Syed, N., Advani, J., Renuse, S., Sahasrabuddhe, N.A., Prasad, T.S., et al., 2017. Silac-based quantitative proteomic analysis reveals widespread molecular alterations in human skin keratinocytes upon chronic arsenic exposure. Proteomics 17 (6).
Moll, R., Divo, M., Langbein, L., 2008. The human keratins: biology and pathology. Histochem. Cell Biol. 129 (6), 705–733.
Natsch, A., Emter, R., 2017. Reaction chemistry to characterize the molecular initiating event in skin sensitization: a journey to be continued. Chem. Res. Toxicol. 30 (1), 315–331.
Nielsen, J.E., Gunner, M.R., García-Moreno, B.E., 2011. The pka cooperative: a collaborative effort to advance structure-based calculations of pka values and electrostatic effects in proteins. Proteins 79 (12), 3249–3259.
OECD, 2014. The Adverse Outcome Pathway for Skin Sensitisation Initiated by Covalent Binding to Proteins.
Pagadala, N.S., Syed, K., Tuszynski, J., 2017. Software for molecular docking: a review. Biophys. Rev. 9 (2), 91–102.
Pamplona, R., 2011. Advanced lipoxidation end-products. Chem. Biol. Interact. 192 (1–2), 14–20.
Parkinson, E., Boyd, P., Aleksic, M., Cubberley, R., O'Connor, D., Skipp, P., 2014. Stable isotope labeling method for the investigation of protein haptenation by electrophilic skin sensitizers. Toxicol. Sci. 142 (1), 239–249.
Parkinson, E., Aleksic, M., Cubberley, R., Kaur-Atwal, G., Vissers, J.P.C., Skipp, P., 2018. Determination of protein haptenation by chemical sensitisers within the complexity of the human skin proteome. Toxicol. Sci.
Parkinson, E., Aleksic, M., Arthur, R., Regufe Da Mota, S., Cubberley, R., Skipp, P.J., 2020. Proteomic analysis of haptenation by skin sensitisers: diphencyprone and ethyl acrylate. Toxicol. In Vitro 62, 104697.
Randall, M.J., Hristova, M., van der Vliet, A., 2013. Protein alkylation by the alpha,beta-unsaturated aldehyde acrolein. A reversible mechanism of electrophile signaling? FEBS Lett. 587 (23), 3808–3814.
Reynolds, J., MacKay, C., Gilmour, N., Miguel-Vilumbrales, D., Maxwell, G., 2019. Probabilistic prediction of human skin sensitiser potency for use in next generation risk assessment. Comput. Toxicol. 9, 36–49.
Robinson, M.K., Nusair, T.L., Fletcher, E.R., Ritz, H.L., 1990. A review of the buehler guinea pig skin sensitization test and its use in a risk assessment process for human skin sensitization. Toxicology 61, 91–107.
Sanderson, P.N., Simpson, W., Cubberley, R., Aleksic, M., Gutsell, S., Russell, P.J., 2016. Mechanistic understanding of molecular initiating events (mies) using nmr spectroscopy. Toxicol. Res. 5 (1), 34–44.
Shevchenko, A., Jensen, O.N., Podtelejnikov, A.V., Sagliocco, F., Wilm, M., Vorm, O., Mortensen, P., Shevchenko, A., Boucherie, H., Mann, M., 1996. Linking genome and proteome by mass spectrometry: large-scale identification of yeast proteins from two dimensional gels. Proc. Natl. Acad. Sci. U. S. A. 93 (25), 14440–14445.
Silva, J.C., Gorenstein, M.V., Li, G.Z., Vissers, J.P., Geromanos, S.J., 2006. Absolute quantification of proteins by lcmse: a virtue of parallel ms acquisition. Mol. Cell Proteomics 5 (1), 144–156.
Simonsson, C., Andersson, S.I., Stenfeldt, A.L., Bergstrom, J., Bauer, B., Jonsson, C.A., Ericson, M.B., Broo, K.S., 2011. Caged fluorescent haptens reveal the generation of cryptic epitopes in allergic contact dermatitis. J. Invest. Dermatol. 131 (7), 1486–1493.
Tyanova, S., Temu, T., Sinitcyn, P., Carlson, A., Hein, M.Y., Geiger, T., Mann, M., Cox, J., 2016. The perseus computational platform for comprehensive analysis of (prote) omics data. Nat. Methods 13 (9), 731–740.
van Och, F.M., Vandebriel, R.J., Prinsen, M.K., De Jong, W.H., Slob, W., van Loveren, H., 2001. Comparison of dose-responses of contact allergens using the guinea pig maximization test and the local lymph node assay. Toxicology 167 (3), 207–215.
Wall, S.B., Smith, M.R., Ricart, K., Zhou, F., Vayalil, P.K., Oh, J.Y., Landar, A., 2014. Detection of electrophile-sensitive proteins. Biochim. Biophys. Acta 1840 (2), 913–922.
Wessel, D., Flugge, U.I., 1984. A method for the quantitative recovery of protein in dilute solution in the presence of detergents and lipids. Anal. Biochem. 138 (1), 141–143.
Wong, H.L., Liebler, D.C., 2008. Mitochondrial protein targets of thiol-reactive electrophiles. Chem. Res. Toxicol. 21 (4), 796–804.
Zhang, X., Yin, M., Zhang, L.J., 2019. Keratin 6, 16 and 17-critical barrier alarmin molecules in skin wounds and psoriasis. Cells 8 (8).